Characteristics of $Zn_{1-x}Al_xO$ NR/ITO Composite Films Oriented Application for Optoelectronic Devices

Nguyen Dinh Lam

***Abstract*— The Zn1-xAlxO nanorod (NR) were grown on ITO substrates by a hydrothermal process. The influences of the Al doping concentration on the surface morphology, structural, optical, and electrical characteristics of the $Zn_{1-x}Al_xO$ NR/ITO composite film were investigated in detail. The results indicated that characteristics of the $Zn_{1-x}Al_xO$ NR/ITO composite film were strongly influenced by the Al doping concentration. Furthermore, the lowest vertical resistance of the $Zn_{1-x}Al_xO$ NR can be obtained when x = 0.01 and it strongly reduces when the concentration of UV light illumination increases. This reduction follows an exponential decay with a decay rate of 4.35. This result shows good photoconductivity response of the $Zn_{1-x}Al_xO$ NR/ITO composite film and its ability to apply for optoelectronic devices material.**

***Index Terms*— $Zn_{1-x}Al_xO$ NR/ITO composite film, Al doping, Optoelectronic devices.**

Original Research Paper
DOI: 10.7251/ELS2024043L

I. Introduction

ZINC oxide (ZnO) is a II-VI semiconductor with attractive characteristics such as a large exciton binding energy of 60 meV and a wide direct bandgap of 3.37 eV [1]-[3]. In application for optoelectronic devices or photocatalytic materials, ZnO material is usually fabricated under one dimension (1D) nanostructures array [4]-[9]. By applying ZnO 1D nanostructure, the performances of solar cell and light emitting diode devices were significantly enhanced compared to that using ZnO film [10]-[11]. This enhancement in the characteristics of these devices was explained due to a higher electrical conductibility and larger effective surface area. Furthermore, optical, structural, and electrical characteristics of the ZnO 1D nanostructures can be also controlled and improved by doping with some kind of materials such as silver, copper, gallium, cerium, yttrium, and etc [12]-[21]. The red-shift in the absorption band of the ZnO nanostructure corresponding to improving the absorption of the photocatalysts was achieved by silver doping [13]-[14]. Besides that, the cerium doped ZnO nanostructure decreased band gap energy from 3.37 eV to 3.18eV, decreased size of nanorods, and increased the green emission peak in photoluminescence spectra [15]-[16]. In addition, Al doped ZnO nanostructures was also enhanced free charge carriers resulting in increasing electrical property [22]-[23]. However, the influences of Al doping concentration on the characteristics of $Zn_{1-x}Al_xO$ nanostructure fabricated under film are still needed further investigation in detail for optoelectronic devices applications.

In this work, wurtzite type $Zn_{1-x}Al_xO$ NR structures were grown on ITO substrates by hydrothermal method (called the $Zn_{1-x}Al_xO$ NR/ITO composite film). Influences of the Al doping concentration on surface morphology, structural, and optical characteristics of the $Zn_{1-x}Al_xO$ NR/ITO composite film were investigated. Furthermore, electrical property of the $Zn_{1-x}Al_xO$ NR/ITO composite film was also evaluated to find out optimized conditions for application in optoelectronic devices fabrication.

II. Experimental Details

The Zn1-xAlxO NR/ITO composite film were fabricated as the following processes. The first step, ITO substrates were immersed in HCl solution for 10 min to remove organic contamination and then cleaned by methanol, and deionized water in sequence. The second step, 0.1 M solution of zinc acetate dehydrate ($Zn(CH_3COO)_2.2H_2O$) was spin coated on the ITO substrates. After the coating process, the zinc acetate dehydrate coated layer on ITO substrates were dried at 150 ^oC for 20 minutes in an oven to evaporate the solvent and remove organic residuals and then annealed at 500 ^oC for 1 h in air environment to create a ZnO seed layer on ITO substrates. The final step, $Zn_{1-x}Al_xO$ NR structures were grown by hydrothermal process with x varied from 0 to 0.03. In this process, ITO substrates with coated ZnO seed layer and 100 mL solution of 20 mM zinc nitrate ($Zn(NO_3)_2.6H_2O$), 5 mM $C_6H_{12}N_4$ and $Al(NO_3)_3.9H_2O$ with various molar concentrations of Al^{3+} (0%, 1%, 2%, and 3% in comparison with molar concentration of Zn^{2+}) were transferred together into Teflon-lined stainless steel autoclave and then baked at 80 ^oC for 2 hours. The growth time, growth temperature, zinc nitrate concentration, and volume of solution were kept as constants. The obtained the $Zn_{1-x}Al_xO$ NR/ITO composite films after growth processes were ultrasonically

Manuscript received 23 December 2019. Received in revised form 1 March 2020. Accepted for publication 4 April 2020.

Nguyen Dinh Lam is with the Faculty of Engineering Physiscs and Nanotechnology, VNU-University of Engineering and Technology, Vietnam National University, Hanoi, Vietnam (phone: +84-902-233-144; email: lamnd2005@gmail.com)

This research is funded b Vietnam National University, Hanoi (VNU) under project number QG.19.20.

cleaned in ethanol and distilled water for 30 min, followed with drying treatment at 100 °C for 1 hours in air environment.

X-ray diffraction patterns of the $Zn_{1-x}Al_xO$ NR/ITO composite film were chartered by an X-Ray Diffractometer (XRD) D5000 with CuKα radiation (λ = 1.5406 Å) at room temperature. The surface morphology of the composite film was observed using a Scanning Electron Microscope (SEM). The optical characteristic of the composite films was studied using an UV–VIS-NIR spectrophotometer in the wavelength range of 300-800 nm at room temperature. The electrical property of the composite films was measured using home-setup system using a Keithley 2000 multimeter and an UV lamp (Hg lamp with a UV bandpass filter).

III. Results And Discussions

SEM images of the $Zn_{1-x}Al_xO$ NR/ITO composite films at various of the Al doping concentrations were shown in Fig. 1.The images show that, $Zn_{1-x}Al_xO$ NRs were of uniform size and have a tendency to become miss oriented perpendicular to the surface of the ITO substrate when the Al doping concentration increases. Furthermore, the diameter, length, and density of the $Zn_{1-x}Al_xO$ nanorod were strongly depended on the Al doping concentrations. The $Zn_{1-x}Al_xO$ NR density dependence was extracted and depicted in Fig.2. This result indicated that, density of the $Zn_{1-x}Al_xO$ nanorod decreases with an increasing of the Al doping concentrations and this reduction follows an exponential function with the decay rate about 0.8. The miss oriented and reduction in $Zn_{1-x}Al_xO$ NR density as increasing of the Al doping concentrations could be attributed to the replacement of bigger Al atoms to Zn position in the crystal lattice.

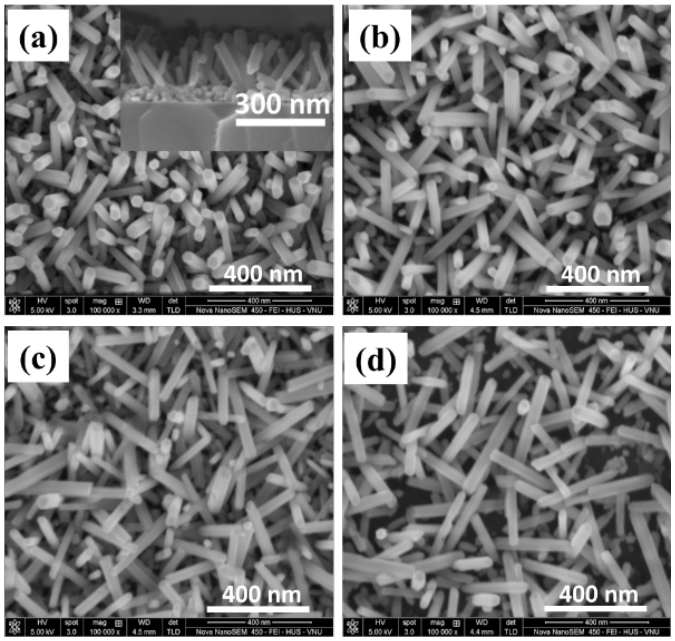

Fig. 1. FE-SEM images of the $Zn_{1-x}Al_xO$ NR/ITO composite films

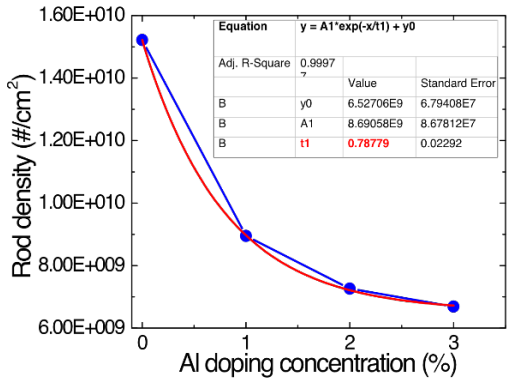

Fig. 2. $Zn_{1-x}Al_xO$ NR density versus the Al doping concentration

The crystal structures of Zn_{1-x}AlxO NR/ITO composite films were characterized by X-ray Diffractometer as shown in Fig.3. All the peaks shown in X-ray diffraction patterns (XRD) were sharp and narrow peaks and closely matched to that of hexagonal wurtzite ZnO structure. Diffraction peaks related to other impurity phases were not observed in the XRD patterns. Furthermore, a small variation of interplaner spacing (dhkl) of Al doped-ZnO from that of ZnO was also observed which implies that aluminum incorporates into ZnO crystal lattice. This means that doping would induce distorted crystal lattice manifested by the displacement of lattice indices. Moreover, the study of the (002) peak intensity also indicated that the ZnO nanorod/ITO structure (x = 0; 0.01) has a preferential orientation along the c-axis. However, when the Al doping concentration increases, this orientation strongly reduces. This is entirely satisfaction with the SEM result as shown in Fig.1. Furthermore, based on the Scherrer's formula of [26], the crystallite size was calculated where d is the crystallite size, λ is the X-ray wavelength (1.54Å), β is the full width at half maximum (FWHM), and θ is the diffraction angle.

$$d = \frac{0.9\lambda}{\beta \cos t} \tag{1}$$

The calculation data indicates that the average grain size was slightly smaller as well as increasing of the Al-doping amount that might be attributed to the substitution of bigger Al atoms at Zn site in the lattice of ZnO [24]-[25].

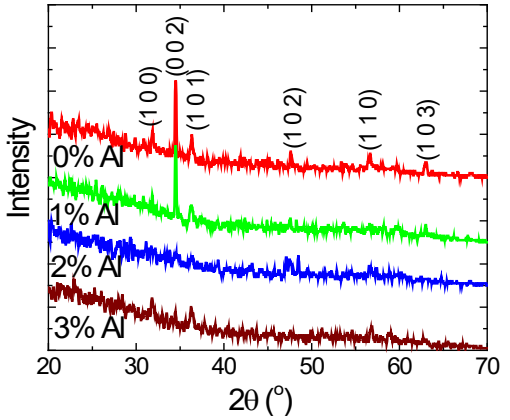

Fig. 3. XRD patterns of the Zn1-xAlxO NR/ITO composite films

According to the diffraction peaks corresponding to planes (1 0 0), (0 0 2), and (1 0 1) the lattice constants were calculated, the results were summarized in table 1.

TABLE I. THE DIMENSIONS OF $Zn_{1-X}AL_xO$ NR STRUCTURE

Sample	FWHM	D(nm)	a(nm)	c(nm)
0% Al	0.488	17.013	0.325	0.523
1% Al	0.368	27.736	0.325	0.520
2% Al	0.410	20.251	0.324	0.521
3% Al	0.443	18.747	0.324	0.520

The influence of the Al doping concentration on the optical characteristics was shown in Fig. 4. The optical transmittance of the $Zn_{1-x}Al_xO$ NR/ITO composite films was slightly depended on the Al doping concentration (Fig. 4.(a)). This can be explained based on the changing of length, density, and orientation of $Zn_{1-x}Al_xO$ NR. However, the optical transmittance of the $Zn_{1-x}Al_xO$ NR/ITO composite films with variation in Al doping concentrations was still higher 95% in visible region with the highest obtained average transmittance of 1% Al doping concentration as shown in Fig. 4.(b). For estimating the band gap energy (Eg) of the $Zn_{1-x}Al_xO$ NR/ITO composite film, the first derivative of the optical transmittance spectra versus wavelength were calculated and presented in Fig. 4.(c). The bandgap energies that correspond to the peaks for all of the structures were extracted and depicted in Fig. 4.(d). The result indicates that the bandgap energy can be slightly enlarged as the higher Al doping concentration. The blue shift of the absorption edge might be attributed to an increase of carrier doping concentration. The doping increases the carrier concentration, when the Zn ions are replaced by Al ions, which may shift the Fermi level leading to widening of bandgap and increase in transmission which called Burstein–Moss effect [27]-[30].

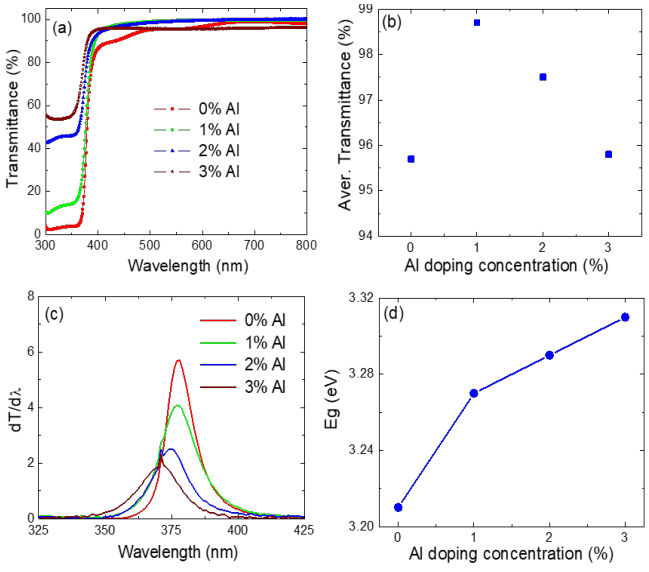

Fig. 4. Optical characteristics of the Zn1-xAlxO NR/ITO composite films

For the electrical property investigation, ITO layer was an electrode. Another electrode was made by silver paste. The I-V characteristics of the $Zn_{1-x}Al_xO$ NR/ITO composite film as shown in Fig. 5 were measured under dark and illuminated by UV lamp. The ohmic and quasi-liner behavior were observed in both of dark and under illumination conditions (Fig. 5.(a, c)). At a given voltage, the current was strongly influenced by the concentration of Al dopant. The highest current was obtained when the Al doping concentration was 1% that resulting in the lowest resistance as shown in Fig. 5.(b). This variation in electrical characteristic of the $Zn_{1-x}Al_xO$ NR/ITO composite film could be attributed to the dependence of NR length, density, and orientation on the Al doping concentration [31]-[33]. The I-V characteristics of the $Zn_{0.99}Al_{0.01}O$ NR/ITO composite film under UV light illumination were measured to find out the photon response of $Zn_{1-x}Al_xO$ NR as shown in Fig. 5.(c). The result indicated that $Zn_{1-x}Al_xO$ NR showed the good photon response when the UV light concentration changes from 0 to 30 mW/cm2. The related resistances were also extracted from Fig. 5.(c) and replotted in Fig. 5.(d). This indicated that the resistance of the $Zn_{1-x}Al_xO$ NR reduces when the UV light concentration increases and following an exponential decay with a decay rate of 4.35. These results indicated that the $Zn_{0.99}Al_{0.01}O$ NR shows good photoconductivity response and its ability to apply for optoelectronic devices material.

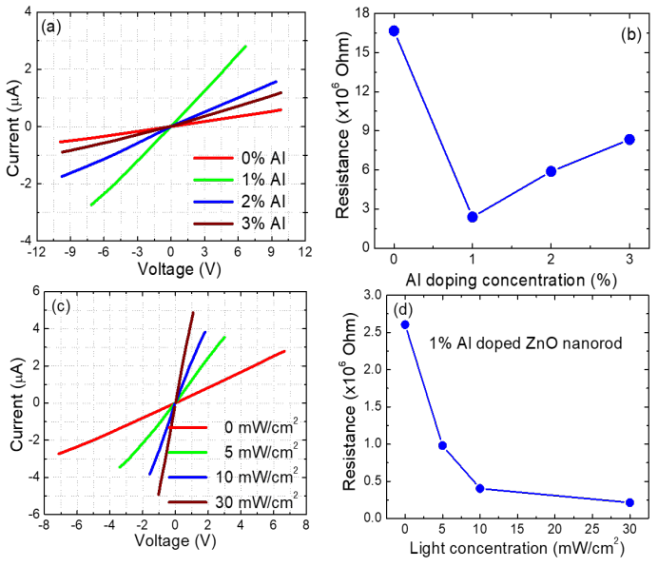

Fig. 5. Electrical characteristics of the Zn1-xAlxO NR/ITO composite films

Based on the NR density as shown in Fig. 2 and electrical characteristics as shown in Fig. 5(b) of the $Zn_{1-x}Al_xO$ samples, the average value of electrical resistance and resistivity of an individual $Zn_{1-x}Al_xO$ NR could be calculated and summarized in Tab. II.

TABLE II. THE AVERAGE VALUE OF ELECTRICAL RESISTANCE AND RESISTIVITY OF AN INDIVIDUAL $Zn_{1-X}AL_xO$ NR

	0% Al	*1% Al*	*2% Al*	*3% Al*
Resistance ($x10^{17}\Omega$)	2.54	0.21	0.43	0.56
Resistivity (Ω.m)	4.25	0.35	0.72	0.92

IV. Conclusion

The influences of the Al doping concentration on the surface morphology, structural, optical, and electrical characteristics of the $Zn_{1-x}Al_xO$ NR/ITO composite films were investigated in detail. When the Al doping concentration increases, the density and orientation along the c-axis of the $Zn_{1-x}Al_xO$ NR were decreased, the bandgap energy was slightly enlarged due to the Burstein–Moss effect. All the $Zn_{1-x}Al_xO$ NR/ITO composite film showed a higher 95% in optical transmittance and the highest of 98.6% was obtained by 1% Al doping concentration. However, the best electrical behavior can be observed by the 1% Al doping concentration. This sample also showed good photoconductivity response and its ability to apply for optoelectronic devices material.

References

[1] Raoufi, D., and Raoufi, T.: "The effect of heat treatment on the physical properties of sol–gel derived ZnO thin films", *Appl Surf Sci*, 2009, 255, pp. 5812–5817

[2] Choppali, U., Kougianos, E., Mohanty, S.P., and Gorman, B.P.: "Polymeric precursor derived nanocrystalline ZnO thin films using EDTA as chelating agent", *Sol. Energy Mater Sol. Cells*, 2010, 94, pp. 2351–2357

[3] Klingshirn, C.: "*ZnO: Material, Physics and Applications*", Chemphyschem., 2007, 8, (6), pp. 782-803

[4] Aravapalli, V., Suresh, M., Jeevanandam, J., Venkatesh, S. K., Gousia, D. P., Balaji, D., and Murthy, N. B.: "Copper-Doped Zinc Oxide Nanoparticles for the Fabrication of white LEDs", *Protection of Metals and Physical Chemistry of Surfaces*, 2019, 55, (3), pp. 481–486

[5] Siddharth, C., Annapoorni, S., and Malik, R.: "Evolution and growth mechanism of hexagonal ZnO nanorods and their LPG sensing response at low operating temperature", *Sensors and Actuators A*, 2019, 293, pp. 207–214

[6] Xing, W., Ran, Y., Ziqiang, J., Tingting, G., Fengni, H., Wei, W., Zifeng, X., and Li, D.: "Cirtopic white LED with a 490 nm emission peak based on He-Zn annealed ZnO nanorods/polymer blend p-n heterojunction", *J. of All. and Comp.*, 2019, 780, pp. 306-311

[7] Mohd, S. A., Hamad A. A., Mahmood, M. S., Zeenat, A., and Sartaj, T.: "Catalytic induced morpholical transformation of porous ZnO to ZnO nanorods by Sn(IV) and their effect on photocatalytic reduction of methylene blue and DFT calculations", *Spectrochimica Acta Part A: Molecular and Biomolecular Spectroscopy*, 2019, 220, pp. 117101

[8] An, K., Kim, J., Afsar. U. M., Rhee, S., Kim, H., Kang, K. T., Young, W. H., and Lee, C.: "Germinant ZnO nanorods as a charge-selective layer in organic solar cells", *Journal of Materials Science and Technology, 2019*, https://doi.org/10.1016/j.jmst.2019.07.027

[9] Dash, P., Manna, A., Mishra, N.C., and Shikha, V.: "Synthesis and characterization of aligned ZnO nanorods for visible light photocatalysis", Physica E: *Low-dimensional Systems and Nanostructures*, 2019, 107, pp. 38-46

[10] Geunchul, P., Soo, M. H., Seung, M. L., Jun, H. C., Keun, M. S., Hyun, Y. K., Hyun-Suk, K., Sung-Jin, E., Seung-Boo, J., Jun, H. L., and Jinho, J.: "Hydrothermally Grown In-doped ZnO Nanorods on p-GaN Films for Color-tunable Heterojunction Light-emitting-diodes", *Scientific Reports*, 2015, 5:10410

[11] Joel, J., Sehoon, C., Patrick, R. B., Jayce, J. C., Paul, H. R., Moungi, G. B., Silvija, G., and Vladimir B.: "ZnO nanowire arrays for enhanced photocurrent in PbS quantum dot solar cells", *Adv. Mater.*, 2013, 25, pp. 2790–2796

[12] Kösemen, A.: "Electrochemical growth of Y doped ZnO nanorods for use in inverted type organic solar cells as electron transport layer", *Mater. Res. Express*, 2019, 6, pp. 095024

[13] Abdus, S., Syed, M. S., and Hazrat, H.: "Band gap tuning and applications of ZnO nanorods in hybrid solar cell: Agdoped verses Nd-doped ZnO nanorods", *Materials Science in Semiconductor Processing*, 2019, 93, pp. 215–225

[14] Hsu, M.H., and Chang, C. J.: "Ag-doped ZnO nanorods coated metal wire meshes as hierarchical photocatalysts with high visible-light driven photoactivity and photostability", *J Hazard Mater.*, 2014, 278, pp. 444-53

[15] Aisah, N., Gustiono, D., Fauzia, V., Sugihartono, I., and Nuryadi, R.: "Synthesis and Enhanced Photocatalytic Activity of Ce-Doped Zinc Oxide Nanorods by Hydrothermal Method*", IOP Conf. Series: Materials Science and Engineering*, 2017, 172, pp. 012037

[16] Sinha, N., Geet, R., Sonia, B., Sanjay, G., Binay, K.: "Synthesis and enhanced properties of cerium doped ZnO nanorods", *Ceramics International, 2014*, 40, (8:A), pp. 12337-12342

[17] Agarwal, D. C., Singh, U. B., Srashti, G., Rahul, S., Kulriya, P. K., Fouran, S., Tripathi, A., Jitendra, S., Joshi U. S., and Avasthi, D. K.: "Enhanced room temperature ferromagnetism and green photoluminescence in Cu doped ZnO thin film synthesised by neutral beam sputtering", *Scientific Reports*, 2019, 9, 6675

[18] Zhou, H., Yang, L., Pengbin, G., Corey, R. G., Zehao, S., Hao, W., and Guojia, F.: "Ga-doped ZnO nanorod scaffold for high-performance, hole-transport-layer-free, self-powered CH3NH3PbI3 perovskite photodetectors", *Solar Energy Materials and Solar Cells*, 2019, 193, pp. 246-252

[19] Goktas, A.: "High-quality solution-based Co and Cu co-doped ZnO nanocrystalline thin films: Comparison of the effects of air and argon annealing environments", *Journal of Alloys and Compounds*, 2018, 735, pp. 2038–2045

[20] Al-Ghamdi, A. A., Al-Hartomy, O. A., El Okr, M., Nawar, A. M., El-Gazzar, S., El-Tantawy, F., and Yakuphanoglu, F.: "Semiconducting properties of Al doped ZnO thin films", *Spectrochimica Acta Part A: Molecular and Biomolecular Spectroscopy*, 2014, 131, pp. 512–517

[21] Tumbul, A., Aslan, F., Demirozu, S., Goktas, A., Kılıç, A., Durgun, M., anf Zarbali, M. Z.: "Solution processed boron doped ZnO thin films: Influence of different boron complexes", *Materials Research Express*, 2018, 6, 035903

[22] Christian, M. P. and Hisao, Y.: "Enhanced Charge Transport in Al-doped ZnO Nanotubes Designed via Simultaneous Etching and Al Doping of H2O-Oxidized ZnO Nanorods for Solar Cell Applications", J. Mater. Chem. C, 2019, DOI: 10.1039/C9TC00401G

[23] Khalid, N.R., Hammad, A., Tahir, M.B., Rafique, M., Iqbal, T., Nabi, G., and Hussain, M.K.: "Enhanced photocatalytic activity of Al and Fe co-doped ZnO nanorods for methylene blue degradation", *Ceramics International*, 2019, https://doi.org/10.1016/j.ceramint.2019.07.132

[24] Yasemin, C., Müjdat, C., and Saliha, I.: "Microstructural, optical and electrical studies on sol gel derived ZnO and ZnO:Al films", *Current Applied Physics*, 2012, 12, pp. 963-968

[25] Jianzi, L., Jian, X., Qingbo, X., and Gang, F.: "Preparation and characterization of Al doped ZnO thin films by sol–gel process*", Journal of Alloys and Compounds*, 2012, 542, pp. 151–156

[26] Mingsong, W., Ka, E. L., Sung, H. H., Eui, J. K., Sunwook, K., Jin, S. C., Eun, W. S., and Chinho, P.: "Optical and photoluminescent properties of sol-gel Al-doped ZnO thin films", *Materials Letters*, 2007, 61, pp. 1118–1121

[27] Shan, F.K., and Yu, Y.S.: "Band gap energy of pure and Al-doped ZnO thin films", *Journal of the European Ceramic Society*, 2004, 24, pp. 1869–1872

[28] Aslan, F., Tumbul, A., Göktaş, A., Budakoğlu, R., and Mutlu, İ. H.: "Growth of ZnO nanorod arrays by one-step sol–gel process", *Journal of Sol-Gel Science and Technology*, 2016, 80, (2), pp. 389–395

[29] Shrisha, B. V., Bhat, S., Kushavah, D., and Gopalakrishna, N.K.: "Hydrothermal growth and characterization of Al-doped ZnO nanorods", *Materials Today: Proceedings*, 2016, 3, (6), pp. 1693–1701

[30] Goktas, A.: "Role of simultaneous substitution of Cu2+ and Mn2+ in ZnS thin films: Defects-induced enhanced room temperature ferromagnetism and photoluminescence", *Physica E: Low-Dimensional Systems and Nanostructures*, 2020, 117, pp. 113828

[31] Gencer, H., Goktas, A., Gunes, M., Mutlu, H. I., and Atalay, S.: "Electrical transport and magnetoresistance properties of $La_{0.67}Ca_{0.33}MnO_3$ film coated on pyrex glass substrate", *Inter. Jour. of Mod. Phys. B*, 2008, 22, (05), pp. 497–506

[32] Gu, X. Q., Zhu, L. P., Cao, L., Ye, Z. Z., He, H. P., and Chu, P. K.: "Optical and electrical properties of ZnO:Al thin films synthesized by low-pressure pulsed laser deposition", *Materials Science in Semiconductor Processing*, 2011, 14 (1), pp. 48–51

[33] Goktas, A., Aslan, F., Yeşilata, B., and Boz, İ.: "Physical properties of solution processable n-type Fe and Al co-doped ZnO nanostructured thin films: Role of Al doping levels and annealing", *Materials Science in Semiconductor Processing*, 2018, 75, pp. 221–233